Robotic Threading from a Gel-like Substance Based on Impedance Control With Force Tracking

Houari Bettahar, P.A. Diluka Harischandra, and Quan Zhou, *Member, IEEE*

***Abstract*—Gel-like matter is used extensively in a wide range of application fields including industrial applications such as the manufactory and assembly of garment and footwear products, soft macro/micro-robotics, medical diagnostics, and drug delivery. However, the manipulation of gel-like matter is very challenging, due to its high deformability, high viscosity, and fast phase changing. In this letter, we propose a novel biomimetic robotic fiber threading approach based on impedance control with force tracking. The highly integrated approach can control the impedance of the fiber during both threading and solidification of the fiber and characterize the mechanical properties of the fabricated fibers in the very same setup without changing parts. The impedance control method has also been adapted in this letter by adding a real-time estimator for continuously estimating the stiffness of the threading force for highly accurate control. The resulted fibers using the proposed approach demonstrates higher performances in all terms of toughness, stiffness, elongation and strength, compared to the traditional velocity controlled fiber fabrication approach.**

***Index Terms*—Robotic and automation, impedance control with force tracking, fiber threading.**

I. Introduction

RECENTLY, the gel-like matter became increasingly attractive due to the commercial significance of products in many application fields. For example, in drug delivery, synthetic mucosa-mimetic hydrogels are recently developed to replace animal experiments in the characterization of mucoadhesive drug delivery systems [1]. In healthcare, hydrogels are used to burn injuries. Injectable hydrogels can produce a scaffold for in situ tissue regrowth and regeneration, where gel manipulation is essential for the betterment of granulation tissue formation and epithelialization [2]. The gel-like matter is also used to fabricate the nanofiber network incorporated with the biological cue in mimicking native articular cartilage [3]. In soft macro/micro-robotics, hybrid polymer hydrogels allow the design of soft biomimetic actuators and sensors with shape-changing [4], and the fabrication of stretchable microfiber strain sensor with beads-on-a-string structure [5].

Manuscript received June 1, 2021; accepted September 22, 2021. Date of publication September 30, 2021; date of current version October 15, 2021. This work was supported by AI spider silk threading (ASSET) in the AIPSE program of the Academy of Finland under Project 317018. This letter was recommended for publication by Associate Editor M. Rakotondrabe and Editor X. Liu upon evaluation of the reviewers' comments. *(Corresponding author: Quan Zhou.)*

The authors are with the Department of Electrical Engineering and Automation, School of Electrical Engineering, Aalto University, 00076 Aalto, Finland (e-mail: houari.bettahar@aalto.fi; diluka.harischandra@aalto.fi; quan.zhou@aalto.fi).

Digital Object Identifier 10.1109/LRA.2021.3116697

However, very little research on manipulating gel-like matter has been done beyond basic gel dispensing and threading, despite all the advancements in soft matter manipulation, including digital microfluidics [6], capillary gripping [7], [8], paper fibers manipulation [9], self-alignment based on water droplet [10], etc. Manipulation of the gel-like matter is highly challenging due to its high deformability, high viscosity, and fast phase changing. Moreover, gel-like matters are pliable combinations of liquids, gases, and solids with many interfaces, exhibiting nonlinear responses, and their properties are strongly affected by thermal fluctuations. Consequently, manipulating gel-like matter needs a good understanding and accurate characterization of its properties. The previous study of the manipulation of gel-like matter has been focused on the threading of silk protein and a large variety of polymer materials to generate artificial fibers. A variety of methods have been used, including wet-spinning [11], dry-spinning [12], electrospinning [13], microfluidic spinning [14], and direct writing [15]. However, the produced artificial fibers are just about one-fifth of the strength and a half in the toughness of natural fibers such as spider silk fiber [16]. One of the reasons is that the fabrication process is usually manual open-loop controlled, or based on velocity or position control without real-time feedback of the fiber properties.

On the other hand, many nature species manipulate materials by exploiting their body structures. Archetypal examples include silk spinning in silkworms and spiders [17], [18]. For example, a spider can perform a sophisticated pultrusion based on exceptionally precise control with advanced biological sensing and actuation. A spider can manipulate silk mechanical properties in real-time to comply with the interaction (pulling) forces, in which protein dope can be continuously transformed into fibers with extraordinary mechanical properties [16]. It is among the strongest and toughest biological materials, outperforming most synthetic polymers and even some metal alloys.

To mimic the threading process of a natural spider to fabricate high-performance artificial fibers, robotic and automation methods can be exploited to control the pulling forces during the fiberization of the gel. The potential benefits could include tuning the mechanical properties of the generated fibers, improving the dexterity of the threading task, and avoiding problems related to instability and safety. Impedance control has been widely identified as an efficient approach for controlling the interaction forces of robots contacting a compliant environment [19]. For example, impedance control has been used for controlling the interaction forces indirectly by selecting the desired impedance dynamics without knowledge of environment parameters (e.g.,

stiffness) [20]. Adaptive impedance control has been used to estimate the parameters of the environment [21], [22–[24], where the user must specify the gain matrix of the adaptation law. However, most previous work on impedance control is dealing with compliant structures at contact. For gel-like materials, they are only compliant with small deformation but are plastic and phase changing during the general manipulation process.

In this paper, we propose a novel biomimetic robotic fiber threading approach based on impedance control with force tracking. The highly integrated approach can control the impedance of the fiber during both threading and solidification of the fiber and characterize the mechanical properties of the fabricated fibers in the very same setup without changing parts. The impedance control method has also been adapted in this paper by adding a real-time estimator for continuously estimating the stiffness of the threading force for highly accurate control. The resulted fibers using the proposed approach demonstrates higher performances in all terms of toughness, stiffness, elongation and strength, compared to the traditional velocity controlled fiber fabrication approach.

The paper is organized as follows. Section II formulates the problem. Section III presents the experimental setup. Section IV describes the modeling and control of the robot-gel system. Section V reports and discusses the obtained experimental results. Finally, Section VI concludes the paper.

II. Problem Formulation

The mechanical properties of fiber material influence its behavior as it is loaded. Some of the typical mechanical properties of fiber material include strength, toughness, elongation, stiffness, etc. The stiffness of the material affects the degree it deflects under a load, and the strength is the property of a material that opposes the deformation or breakdown of material in the presence of load forces. The elongation-to-break is the deformation of a sample when it breaks.

Toughness is the most remarkable property of biological materials. It is the capability of a material to consume the energy and gets deformed without breaking up. The value of the toughness of a material can be determined by stress-strain or force-extension characteristics of a material. Because every mechanical system is exposed to loads during operation, it is essential to understand the behavior of materials that build those mechanical systems [25]. Typically, the mechanical properties of a material can be determined using a stress-strain or force-extension curve as shown in Fig. 1.

The force-extension curve can be obtained by gradually applying load force, which can be tensile, compressive, or torsional, on the material and measuring the deformation, from which the force-extension curve can be determined. This curve can reveal many properties of a material. In this section, we are interested in studying the mechanical properties of artificial fibers, especially stiffness and toughness, by applying a tensile force to the gel material.

The proposed threading procedure is illustrated in Fig. 2, consisting of both the gel fiber fabrication and characterization phases, and the corresponding pulling trajectory is illustrated in Fig. 3. In the fiber fabrication phase, especially during pulling

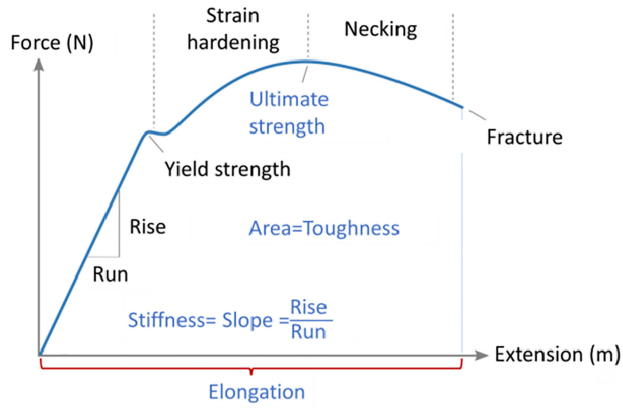

Fig. 1. Force–extension curve, obtained by increasingly applying tensile force and measuring the extension. The first linear region is the elastic region, where the force is proportional to the extension and the slope is stiffness. The end of the region is the initiation point of plastic deformation. The force component of this point is defined as yield strength. The second region is the strain hardening. It begins as the force goes behind the yielding point, achieving a maximum at the ultimate strength point, which is the maximal force that can be achieved and is called the ultimate strength. The third region is the necking. A neck develops after the ultimate strength where the local cross-sectional area gets significantly smaller than the average. The necking will increase as the force concentrates more at a small section, which leads to fracture.

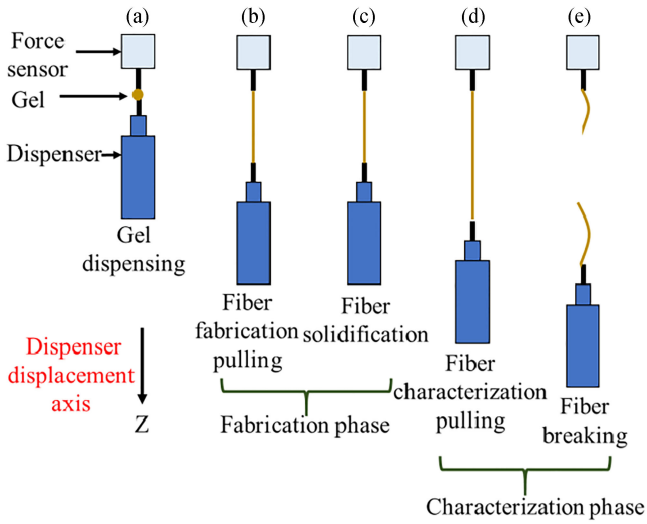

Fig. 2. The proposed threading procedure. (a) a droplet of gel is dispensed between the tip of the force sensor and the dispenser nozzle; b) the dispenser is moved away from the force sensor pulling the gel droplet into a fiber until certain criteria are satisfied, e.g., displacement or force; (c) the system stalls for a certain amount of time to allow the fiber to solidify; (d) the fiber is pulled further until (e) the fiber breaks.

(referred to as fabrication pulling, and the force is referred to as fabrication force), different pulling velocities are applied. To understand the behavior of the pulling force with no pulling motion (referred to as solidification force), the system is kept steady for five minutes while the fiber is solidifying. In the fiber characterization phase, the fiber is pulled again (referred to as characterization pulling, and the force is referred to as characterization force) to investigate the mechanical properties of the fabricated fibers using the force-extension curve after the fiber fabrication phase.

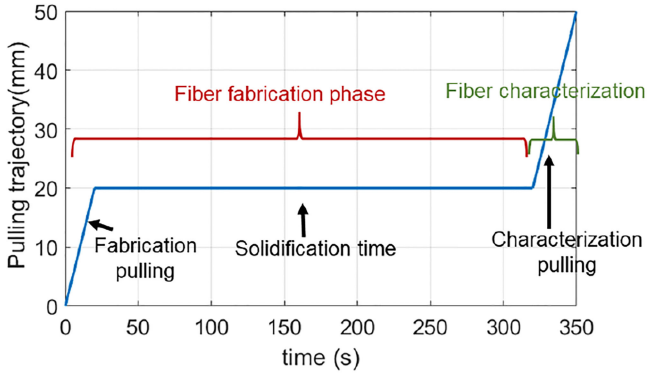

Fig. 3. The proposed pulling trajectory for fiber fabrication and characterizations. In the fiber fabrication phase, the gel is pulled continuously and increasing until a given position, where the fiber solidifies for a given solidification time. Then, the fiber characterization phase starts by pulling continuously and increasing until it breaks.

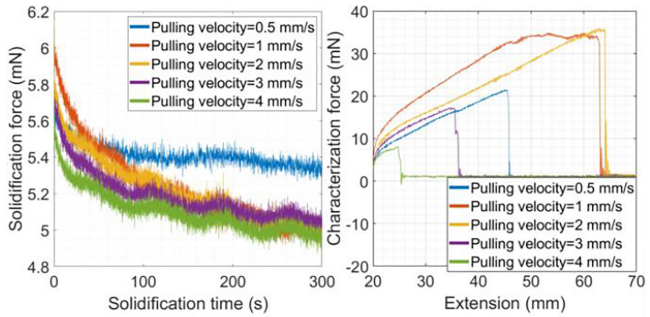

Fig. 4. (a) The solidification force decays during the solidification phase for the four different experiments with different velocities, (b) different characterization force-extension curves are obtained for different fabrication pulling velocities during characterization.

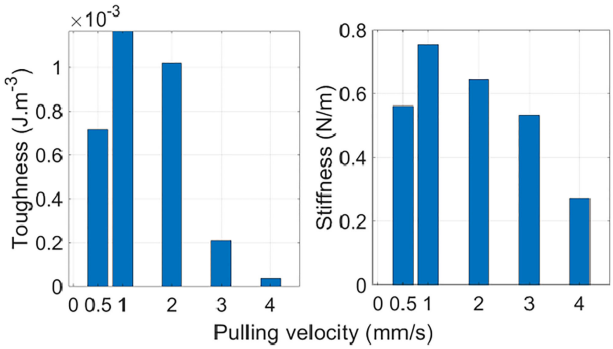

Fig. 5. The calculated toughness and stiffness using Fig. 4(b) for five different experiments with five different fabrication pulling velocities. The toughness and the stiffness are higher when the fabrication pulling velocity is smaller.

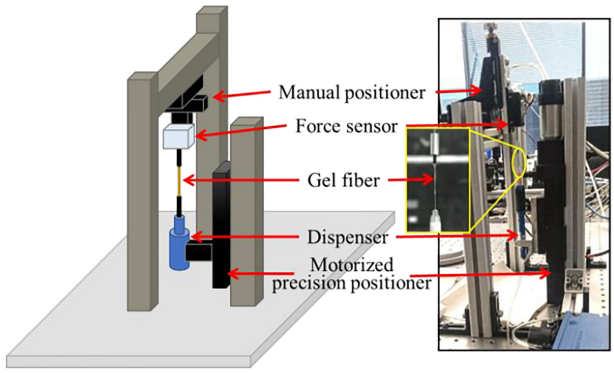

Fig. 6. Robotic experimental setup. The gel dispenser is fixed on a motorized precision positioner, where the force sensor is fixed.

After fabrication pulling the fiber using five different velocities, 0.5, 1, 2, 3, and 4 mm/s, the obtained forces for each velocity during a constant solidification time of five minutes without any pulling motion is shown in Fig. 4(a). We can notice that the solidification forces decrease during this time, which implies that the mechanical properties of the generated fiber change with time.

Fig. 4(b) shows the characterization force as a function of the extension during the characterization phase with different fabrication pulling velocities. This figure shows that the fabricated fibers have different mechanical properties, where the stiffness and toughness are higher for the smaller fabrication pulling velocities (see Fig. 5). Based on the obtained results, we aim at using robotic and automation to control the fabrication force to improve the mechanical properties of the generated artificial fibers. For this sake, impedance control with force tracking is proposed in this paper.

III. Experimental Setup

To implement impedance control with force tracking for our robotic threading (gel pulling), the experimental setup shown in Fig. 6 is employed. The setup, placed on a vibration isolation table, consists of a dispenser (Nordson EFD, model Performus V) held on a motorized precision positioner (Physik Instrumente, model M404.4PD) to dispense and pull the gel. In the rest of the paper, the dispenser with the precision positioner is called robot manipulator. A needle is held on a force sensor (LCM Systems, model LCM UF1), which is fixed, to sense the pulling force after contacting the gel-like substance. The motorized precision positioner is controlled via a controller (Physik Instrumente, model C-884.4CD) using Matlab/Simulink. The measurement of the force sensor is acquired using a data acquisition (DAQ) board (National Instrument, model PCIe-6363). The dispenser is controlled also via the DAQ board.

In the experiments, a commercial fast-curing contact adhesive (Pattex), which is a solvent based polychloroprene rubber, is used to generate artificial fibers by pulling.

IV. System Modeling and Control

The main objective of the modelling and control section is to control the pulling force based on impedance control. For this purpose, the modeling of fiber threading system is required, as well as the development of the control law based on the impedance control.

A. Fiber Threading Model

Fiber threading is the process of pulling the gel to be transformed from a liquid to semi-solid, producing an elastic gel fiber. For the purpose of modeling the fiber threading system, the gel fiber is treated as second-order mass-spring-damper

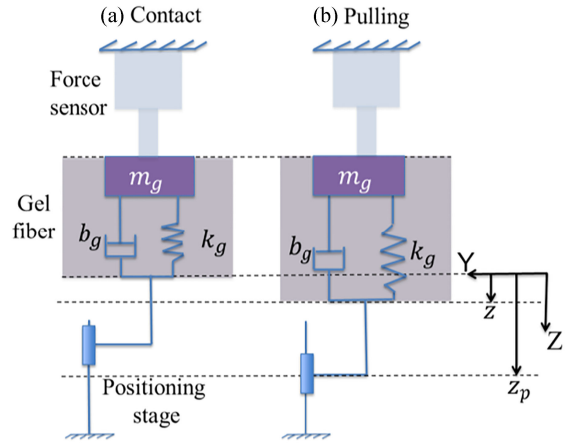

Fig. 7. Fiber threading system model based on mass-spring-damper: (a) just at contact $f_g = 0$ and (b) contact with $f_g \neq 0$.

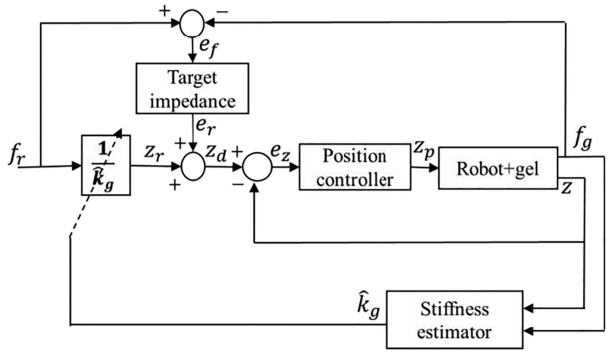

Fig. 8. The impedance control with force tracking control scheme applied on fiber threading during the fabrication phase.

systems. The fiber threading system at contact and after contact is illustrated in Fig. 7. The mass is the gel fiber mass, the spring describes the gel fiber stiffness, and the damping describes the gel fiber viscosity.

During the fabrication pulling process, the properties of the gel change continuously in terms of stiffness, damping as well as mass. Therefore, all three parameters are variables with respect to time. In Fig. 7, the force applied by the robot end-effector on the gel material is given by:

$$m_g(t)\,\ddot{z} + b_g(t)\,\dot{z} + k_g(t)\,z = f_g \tag{1}$$

where $m_g(t)$, $b_g(t)$ and $k_g(t)$ are respectively the mass, damping, and stiffness of the gel.

z is the current position of the tip of the robot manipulator. f_g is the current fabrication force applied by the robot manipulator end effector to the gel once contact between both is established. In this paper, z_p is the output of the block "Position controller" (see Fig. 8), and f_g is the pulling force to be controlled based on impedance control, as described in the next subsection.

B. Impedance Control With Force Tracking Under Variable Stiffness

Impedance control has been widely classified as an efficient approach for compliant control of robots contacting the environment. Its objective as introduced in [26] is to provide a desired user-specified dynamical relationship, referred to as, target impedance or impedance filter, between the robot end-effector position z and the fabrication force f_g. Typically, the target impedance is selected as a linear second-order system, so that the dynamical relationship between the fabrication force f_g and the end effector position z can be controlled by a mass-spring-damper system.

A common mathematical description of the target impedance is given by (2), where M, B and K are respectively the desired mass, damping and stiffness of the target impedance, z_r is the reference position, f_r is the reference force and e_f is the force error.

$$M\left(\ddot{z} - \ddot{z}_r\right) + B\left(\dot{z} - \dot{z}_r\right) + K\left(z - z_r\right) = f_r - f_g = e_f \tag{2}$$

The position controller can be implemented using the proportional-integral-derivative (PID) controller. Thus, the control law can be expressed as

$$z_p = k_p\, e_z + k_i \int e_z + k_v \dot{e}_z \tag{3}$$

where $k_p, k_i,$ and k_v are the PID controller gains, where $e_z = z_d - z$, represents the position error between the desired generated position and the current position.

The position tracking error, due to the dynamics of the robot, will occur between the end-effector position and the desired position calculated by (2). In this case, (2) can be rewritten as in (4):

$$M\ddot{e}_r + B\dot{e}_r + Ke_r = f_r - f_g = e_f \tag{4}$$

where $e_r = z_d - z_r$. Once the force f_g enters the steady state (after the transient time), the velocity has little changes, hence the inertia and the viscose force are mostly constant. Therefore, the gel stiffness is the most dominant deformation, and the interaction force in (1) can be written as:

$$k_g(t)\, z \cong f_g \tag{5}$$

The above equation can be rewritten to obtain the robot end-effector position as follows:

$$z = \frac{f_g}{k_g(t)} \tag{6}$$

Inserting the force error in (6) gives

$$z = \frac{f_r - e_f}{k_g(t)} \tag{7}$$

with $e_f = (f_r - f_g)$.

Because the goal of the position controller is to track the desired position reference z_d, a position error can be generated. Accordingly, z_d can be written as:

$$z_d = e_z + \frac{f_r - e_f}{k_g(t)} \tag{8}$$

Substituting (8) in (4) gives the following force/position error differential equation (in closed-loop):

$$M\ddot{e}_f + B\dot{e}_f + (K + k_g(t))\, e_f = M\ddot{f}_r + B\dot{f}_r + Kf_r + k_g(t)\left(M\ddot{e}_z + B\dot{e}_z + K\left(e_z - z_r\right)\right) \tag{9}$$

If the system achieves the steady-state assuming that the desired fabrication force is constant, with $\dot{e}_z = \ddot{e}_z = \dot{e}_f =$

$\ddot{e}_f = \dot{f}_r = \ddot{f}_r = 0$, the steady-state force error can be derived from (9) as:

$$e_f^{ss} = k_{eq}\left[\frac{f_r}{k_g(t)} + e_z - z_r\right] \tag{10}$$

where $k_{eq} = \frac{Kk_g(t)}{K+k_g(t)}$ is the equivalent stiffness of the target impedance and the gel material. The (10) means that if the control law of the position controller is used to reach a zero steady-state position error ($e_z \to 0$) and the reference position is selected precisely, then the steady-state force error will tend towards zero ($e_f^{ss} \to 0$). This leads to:

$$z_r = \frac{f_r}{k_g(t)} \tag{11}$$

The (11) means that if the exact value of the gel stiffness $k_g(t)$ are known, then a reference position z_r could be achieved according to (11), by applying the reference fabrication force f_r on the gel. However, in practice the value $k_g(t)$ is not perfectly known and consequently, the desired force f_r will not be applied on the gel accurately.

To achieve impedance control with force tracking scheme, the gel stiffness $k_g(t)$ should be estimated, because the stiffness of the gel material changes continuously during the threading (fiber pulling). An online estimation method is used to estimate the stiffness $k_g(t)$ during the whole threading process. The proposed estimation method is simple to implement, does not require to define adaptive gains, and requires only data on the location of the robot end-effector and the pulling forces.

The idea is to apply the impedance control law using initial assumption $\hat{k}_g^0$ of k_g. Once the control law is applied, a transition between non-pulling (at contact) and pulling occurs. During this transition, the force and position measurements are recorded.

The gel stiffness is then estimated using the static part of the (1):

$$\hat{k}_g = \frac{f_g}{z}\ if\ z \succ 0 \tag{12}$$

Note that neglecting the dynamic part of the (1) could change the desired dynamic of the system but it will not influence the steady-state part. Using (11), we can rewrite:

$$z_r = \frac{f_r}{k_g} = \frac{f_r}{f_g}\ z \tag{13}$$

The (13) means that if z tracks z_r, then f_g will track f_r. The complete impedance control with force tracking scheme used in this work is shown in Fig. 8.

V. Stability Analysis

Assuming a constant mass and damper with time-varying spring and considering the following positive definite Lyapunov function:

$$V = \frac{1}{2}\ m_g\dot{z}^2 + \frac{1}{2}k_g(t)\ z^2 \tag{14}$$

Take the derivative of (14) and substituting (1) into it leads to:

$$\dot{V} = f_g\ \dot{z} + \left(\frac{1}{2}\dot{k}_g(t)\ z^2 - b_g\dot{z}^2 - k_g(t)\ \dot{z}\right) \tag{15}$$

Accordingly, the following inequality can be concluded:

$$\dot{V} = f_g\ \dot{z} - b_g\dot{z}^2 + \frac{1}{2}\dot{k}_g(t)\ z^2 \leq f_g\dot{z} \tag{16}$$

By assuming slowly varying stiffness, integrating the last equation, to get the following passivity condition:

$$V(t) - V(0) \leq \int_0^t f_g(\tau)\ \dot{z}(\tau)\ d\tau \tag{17}$$

Passivity ensures a stable behavior of the system both in free motion and in case of interaction with, possibly unknown, passive environments [27].

VI. Experimental Results

All the experiments have been done under a constant environmental condition: temperature and relative humidity of 24 °C and a 63% respectively. The force sensor (LCM Systems, model LCM UF1) is based on strain gauges, it returns a signal proportional to the mechanical force applied for the gel pulling. It has a resolution of 0.05 g and an estimated stiffness of 8×10^3 N/m. Impedance control with force tracking performances are described in the next subsection.

A. Impedance Control With Force Tracking Performances

In this section, the impedance control with the force tracking scheme presented in Fig. 8 is implemented, with a sampling frequency of 100 Hz without any knowledge of the stiffness of the gel before pulling. The estimation method presented in Section IV is used to estimate k_g. The impedance control with the force tracking control scheme was evaluated using the experimental setup presented in Section III.

To test the impedance control with the force tracking scheme, a commercial fast-curing contact adhesive has been used.

The PID parameters of the position controller and the target impedance in Fig. 8 have been tuned based on trial-error method, to achieve the desired controlled force performances (time response, accuracy, and overshoot cancelation).

Initial value $\hat{k}_g^0$ is used as an assumption k_g. When $z_r = \frac{f_r}{\hat{k}_g^0} > 0$, the contact to the gel appears and the parameters are estimated, and the force reference is tracked. Once a reference force f_r is applied, the impedance controller takes over and tracks f_g to f_r.

The performance of the impedance control with force tracking is shown in Fig. 9. Note that in Fig. 9 f_g is plotted from the original experimental data, and f_{gf} is plotted after zero-phase filtering. In the rest of the paper, only the filtered forces will be plotted.

As shown in Fig. 9 at contact at time zero, a force is detected. A reference force is set to 2 mN at t = 0 s. The estimation of the stiffness begins, and the impedance controller can track the force reference with a response time of 15 s without overshoot, with a force tracking error of 0.0190 mN (0.95%) and a position error of 0.0053 mm (0.23%). And the stiffness of the gel is estimated continuously during control to be around 0.8671 N/m average. To test the capability of the impedance controller and the effectiveness of the parameter estimation technique, another force reference of 5 mN is applied at t = 50 s. The impedance controller can eliminate the steady-state force error in 13 s

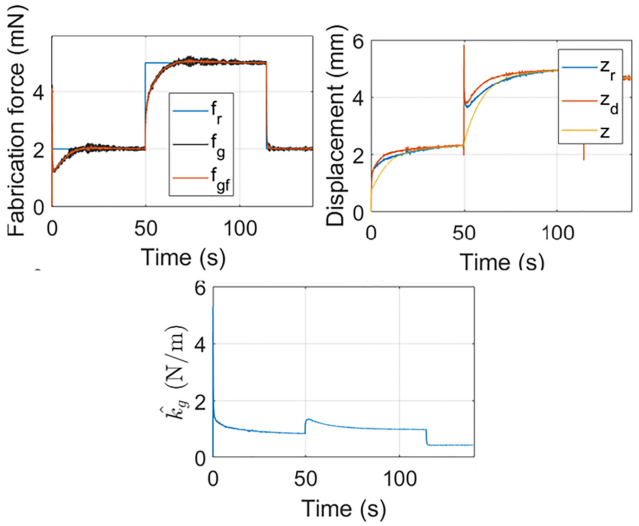

Fig. 9. Impedance control with force tracking with an unknown and variable stiffness of the gel during threading. Fabrication force f_g is compared relative to the force reference f_r. The position of the gel z is compared to the reference z_r and the desired z_d positions. The gel estimated stiffness $\hat{k}_g$ is presented.

without overshoot. The controller is tested in the other direction i.e., if the force reference decreases from 5 mN to 2 mN. The controller can effectively eliminate the steady-state force error in 3 s without overshoot. The absence of the overshoot is very important because the gel is very liquid just after being dispensed, an overshoot force in fabrication pulling can destabilize the system (precision positioning-force sensor-gel), which may disconnect the gel from the force sensor, leading to no force measurements and consequently control failure. For this reason, we designed the controller so that the closed loop system has enough low response time to avoid overshoot and instability.

B. Gel Threading Based on Impedance Control With Force Tracking

Conventionally, the fiber fabrication. i.e., fiber pulling and solidification phases, are based on velocity or position control, where the pulling force profile is not controlled.

For illustration, a fiber fabrication based on velocity control is achieved experimentally. The pulling velocity is 1 mm/s, the best performing fabrication velocity based on earlier tests (see Figs. 4 and 5). The corresponding pulling displacement and applied force profile without control during the fabrication process, as well as the recorded pulling displacement and force during fiber characterization, are shown in Fig. 10. Consequently, during the solidification phase, the force is drifting with time, which leads to the reduction of the final fiber mechanical properties (as explained in Section II).

To improve the mechanical properties of the fabricated fibers, the impedance control with force tracking has been applied in the fiber fabrication phase including fabrication pulling and solidification (see Fig. 2). The applied controlled fabrication force profile based on impedance control is shown in Fig. 11. The corresponding fabrication pulling displacement z is compared

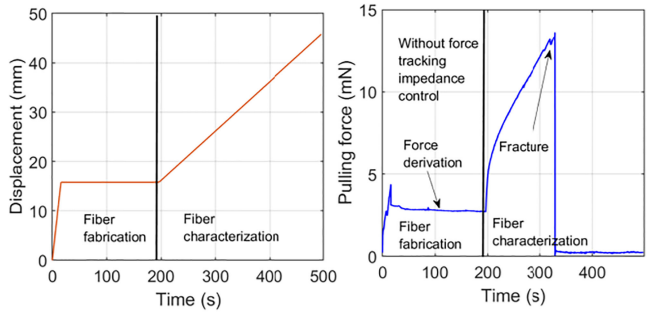

Fig. 10. The pulling displacement and applied force profile during the fabrication process, as well as the recorded puling displacement and force during fiber characterization, based on velocity control.

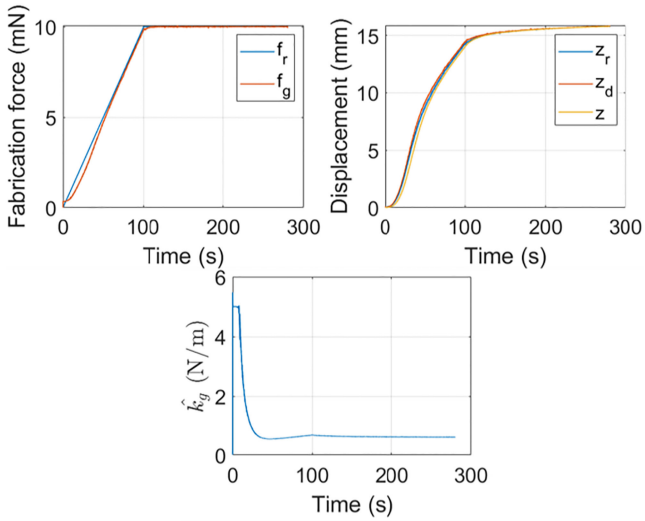

Fig. 11. Impedance control with force tracking for fiber fabrication. The fabrication force f_g is compared with the reference force f_r. The fabrication pulling displacement z is compared to the reference z_r and the desired displacement z_d. The corresponding estimation of gel stiffness during threading $\hat{k}_g$ is presented.

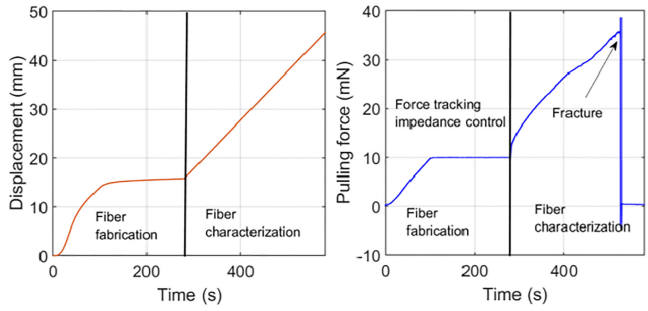

Fig. 12. The pulling displacement and the applied force profile during the fabrication process, as well as the recorded puling displacement and force during fiber characterization, based on impedance control with force tracking.

to the reference displacement z_r and the desired displacement z_d. The estimation of gel stiffness during pulling $\hat{k}_g$ is shown.

After the fabrication process, fiber characterization is done by characterization pulling until the fiber breaks. The pulling displacement and the force profiles during both the fabrication and characterization phases are shown in Fig. 12.

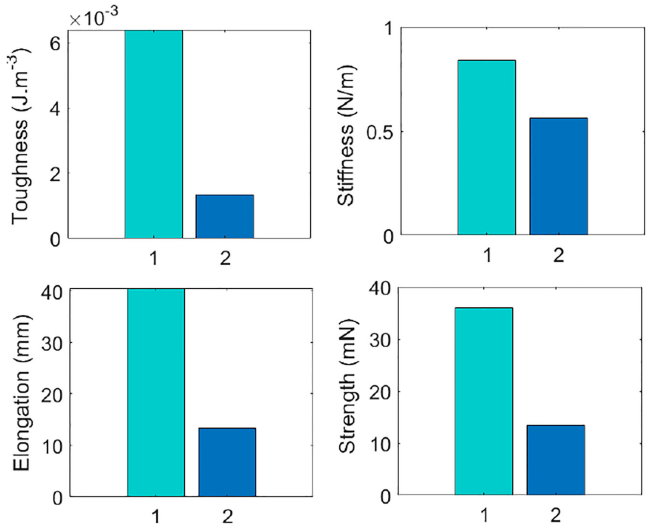

Fig. 13. The obtained mechanical properties: toughness, stiffness, elongation, and strength, for fiber fabrication based on impedance control with force tracking (1) and velocity control (2).

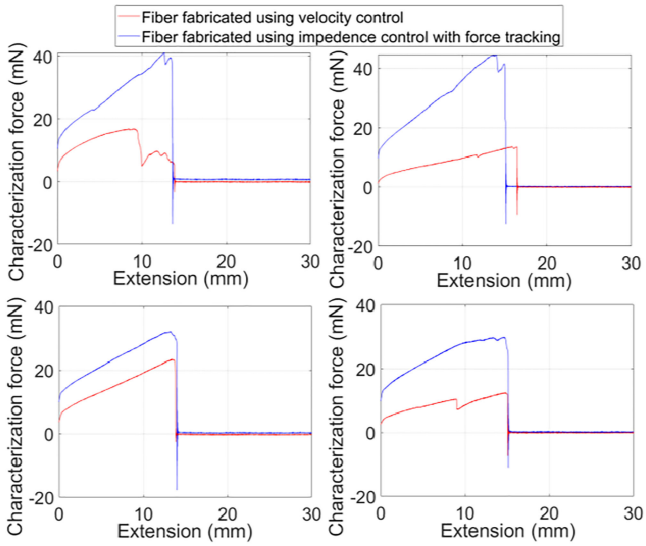

Fig. 14. Mechanical properties comparison of the fabricated fibers. The red color represents the obtained characterization force from fiber characterization after fiber fabrication based on velocity control. And the blue color represents the obtained characterization force from fiber characterization after fiber fabrication based on impedance control with force tracking.

To compare the fiber performances based on velocity control and impedance control with force tracking, we firstly apply the impedance control during the fabrication pulling and solidification of the fibers. The resulted final pulling displacement from the impedance control is used as the final displacement for fabricating a new fiber using velocity control, to achieve the same pulling displacement for the two control approaches allowing a fair comparison. To have a relatively fair comparison, the actual velocity value used in the velocity control is 1 mm/s, the best performing fabrication velocity based on earlier tests (see Figs. 4 and 5).

In Figs. 10 and 12, the pulling displacement and the corresponding pulling force are plotted as a function of time for the two fiber fabrication methods based on velocity control and impedance control with force tracking, respectively. The fabrication pulling time and solidification time for both methods can also be found in the figures. The solidification time is the same for both fiber fabrication methods, which is 180 s. The fabrication pulling time for velocity controlled pulling is 15.8 s, where the pulling time is 100 s for fiber fabrication based on impedance control with force tracking. The obtained fibers are consequently characterized to investigate their mechanical properties.

The obtained mechanical properties: toughness, stiffness, elongation, and strength, for fiber fabricated based on impedance control with force tracking (1) and velocity control (2) are shown in Fig. 13. The obtained toughness, stiffness, elongation, and strength of the fabricated fiber using impedance control with force tracking are (78.89%), (33.00%), (67.11%), and (62.54%) respectively higher than the fabricated fiber using velocity control. The obtained fabricated fiber using impedance control with force tracking gives a toughness, stiffness, elongation, and strength of 6.39×10^{-3} J $\cdot$ m^{-3}, 0.84 $\frac{N}{m}$, 40.56 mm, and 35.93 mN respectively. The obtained fiber toughness, stiffness, elongation, and strength, using velocity control, which gives a toughness, stiffness, elongation, and strength of 1.34×10^{-3} J $\cdot$ m^{-3}, $0.56\frac{N}{m}$, 13.34 mm, and 13.46 mN respectively. The higher mechanical properties of fibers fabricated based on impedance control with force tracking can be explained by the fact that the pulling force during the solidification time is controlled to be constant, unlike fiber fabrication based on velocity control where the pulling force drifts during the solidification time due to a non-control of the pulling force.

To investigate the reproducibility of the high fiber performances using impedance control with force tracking compared to velocity control, several iterations have been done. For each iteration, fiber fabrication based on impedance control with force tracking is firstly done, where the obtained final pulling displacement is used for a new reference displacement for fiber fabrication based on velocity control. In Fig. 14, four iterations are shown. The red color represents the characterization force after fiber fabrication based on velocity control. The blue color represents the characterization force after fiber fabrication based on impedance control.

We can notice that the fabricated fibers based on impedance control with force tracking have significantly higher mechanical performances compared to the fabricated fibers based on velocity control in all iterations. Even through the performances between each subfigure of Fig. 14 are not directly comparable, the reproducibility of higher performance fiber using the proposed technique is evident.

VII. Conclusion

The gel-like matter is highly attractive in a wide range of application fields. However, gel-like matter manipulation is very challenging, due to high deformability, high viscosity, and fast phase changing. In this paper, to mimic the threading process of a natural spider to fabricate high-performance artificial fibers,

robotic and automation methods have been exploited to control the pulling forces during the fiberization of the gel. A robotic fiber threading approach has been proposed based on impedance control with force tracking. For this sake, an experimental setup has been proposed. The proposed impedance control with force tracking method estimates the stiffness using only force and position measurements during the whole threading process. The obtained force tracking error is 0.019 mN (0.95%) and the position error is 0.0053 mm (0.23%). The proposed approach fabricates a high-performance artificial fiber with the desired mechanical properties compared to the classical approaches such as fiber fabrication based on velocity control.

REFERENCES

[1] M. Avijgan, M. Alinaghian, and M. H. Esfahani, "Aloe vera gel as a traditional and complementary method for chronic skin burn: A case report," *Adv. Infect. Dis.*, vol. 7, no. 01, p. 19, 2017.

[2] D. R. Griffin *et al.*, "Accelerated wound healing by injectable microporous gel scaffolds assembled from annealed building blocks," *Nature Mater.*, vol. 14, no. 7, pp. 737–744, 2015.

[3] J. M. Coburn *et al.*, "Bioinspired nanofibers support chondrogenesis for articular cartilage repair," *Proc. Nat. Acad. Sci.*, vol. 109, no. 25, pp. 10012–10017, 2012.

[4] C. Kim *et al.*, "Highly stretchable, transparent ionic touch panel," *Science*, vol. 353, no. 6300, pp. 682–687, 2016.

[5] Z. Liu *et al.*, "Surface strain redistribution on structured microfibers to enhance sensitivity of fiber-shaped stretchable strain sensors," *Adv Mater*, vol. 30, no. 5, 2018, Art. no. 1704229.

[6] J. Zhai *et al.*, "A digital microfluidic system with 3D microstructures for single-cell culture," *Microsystems Nanoeng.*, vol. 6, no. 1, pp. 1–10, 2020.

[7] B. Chang *et al.*, "Capillary transport of miniature soft ribbons," *Micromachines*, vol. 10, no. 10, p. 684, 2019.

[8] M. Cavaiani *et al.*, "Multi-scale 3D printed capillary gripper," in *Proc. Int. Conf. Manipulation, Automat. Robot. Small Scales*, 2018.

[9] J. Hirvonen, "Computer vision measurements for automated microrobotic paper fiber studies," 2017.

[10] V. Sariola, M. Jääskeläinen, and Q. Zhou, "Hybrid microassembly combining robotics and water droplet self-alignment," *IEEE Trans. Robot.*, vol. 26, no. 6, pp. 965–977, Dec. 2010.

[11] A. Koeppel and C. Holland, "Progress and trends in artificial silk spinning: A systematic review," *ACS Biomaterials Sci. Eng.*, vol. 3, no. 3, pp. 226–237, 2017.

[12] C. Fu, Z. Shao, and V. Fritz, "Animal silks: Their structures, properties and artificial production," *Chem. Commun.*, no. 43, pp. 6515–6529, 2009.

[13] J. Xue *et al.*, "Electrospinning and electrospun nanofibers: Methods, materials, and applications," *Chem. Rev.*, vol. 119, no. 8, pp. 5298–5415, 2019.

[14] Y. Jun *et al.*, "Microfluidic spinning of micro-and nano-scale fibers for tissue engineering," *Lab a Chip*, vol. 14, no. 13, pp. 2145–2160, 2014.

[15] H. Chen *et al.*, "Direct writing electrospinning of scaffolds with multidimensional fiber architecture for hierarchical tissue engineering," *ACS Appl. Mater. Interfaces*, vol. 9, no. 44, pp. 38187–38200, 2017.

[16] M. Andersson *et al.*, "Biomimetic spinning of artificial spider silk from a chimeric minispidroin," *Nature Chem. Biol.*, vol. 13, no. 3, pp. 262–264, 2017.

[17] H. Tao, D. L. Kaplan, and F. G. Omenetto, "Silk materials–a road to sustainable high technology," *Adv Mater*, vol. 24, no. 21, pp. 2824–2837, 2012.

[18] T. D. Sutherland *et al.*, "Insect silk: One name, many materials," *Annu. Rev. Entomol.*, vol. 55, pp. 171–188, 2010.

[19] H. F. Al-Shuka *et al.*, "Active impedance control of bioinspired motion robotic manipulators: An overview," *Appl. Bionics Biomech.*, vol. 2018, 2018.

[20] H. Seraji and R. Colbaugh, "Force tracking in impedance control," *Int. J. Robot. Res.*, vol. 16, no. 1, pp. 97–117, 1997.

[21] S. K. Singh and D. O. Popa, "An analysis of some fundamental problems in adaptive control of force and impedance behavior: Theory and experiments," *IEEE Trans. Rob. Autom.*, vol. 11, no. 6, pp. 912–921, Dec. 1995.

[22] S. Misra and A. M. Okamura, "Environment parameter estimation during bilateral telemanipulation," in *Proc. 14th Symp. Haptic Interfaces for Virtual Environ. Teleoperator Syst.*, 2006.

[23] W. Xu *et al.*, "Time-varying force tracking in impedance control," in *Proc. IEEE 51st IEEE Conf. Decis. Control*, Maui, HI, USA, 2012, pp. 344–349.

[24] B. Komati, C. Clévy, and P. Lutz, "Force tracking impedance control with unknown environment at the microscale," in *Proc. IEEE Int. Conf. Robot. Automat.*, Hong Kong, China, 2014, pp. 5203–5208.

[25] A. Lavakumar, "Mechanical properties of materials," in *Concepts in Physical Metallurgy*. San Rafael, CA, USA: Morgan & Claypool, 2017, ch. 5, pp. 5-1–5-22.

[26] N. Hogan, "Impedance control: An approach to manipulation," in *Proc. Amer. Control Conf.*, 1984.

[27] C. Yang *et al.*, "Lyapunov stability and strong passivity analysis for nonlinear descriptor systems," *IEEE Trans. Circuits Syst. I: Regular Papers*, vol. 60, no. 4, pp. 1003–1012, Apr. 2013.